Dilution and non-Fermi-liquid effects in the CePtIn Kondo lattice

F C Ragel[1, 2, #] **, P de V du Plessis**[1, 2] **and A M Strydom**[2]

[1] School of Physics, University of the Witwatersrand, Private Bag 3, PO WITS 2050, Johannesburg, South Africa.
[2] Physics Department, University of Johannesburg, P.O. Box 524, Aucklandpark 2006, South Africa.

E-mail: chalmusragel@seu.ac.lk

Abstract. Measurements of electrical resistivity ($\rho(T)$), magnetoresistivity (MR), magnetic susceptibility ($\chi(T)$) and heat capacity ($C_P(T)$) are presented for the ($Ce_{1-x}La_x$)PtIn alloy system of which the CePtIn parent is a known dense Kondo compound that does not order magnetically down to 50 mK. $\chi(T)$ for alloys $0 \le x \le 0.8$ exhibits Curie–Weiss behaviour. $\rho(T)$ results indicate a transition from a dense Kondo behaviour for $0 \le x \le 0.2$ to a single–ion Kondo region ($0.3 \le x \le 0.8$). The Kondo energy scale as given by T_K values calculated from MR studies and by the temperature $T_{max}^{\rho(mag)}$ where the magnetic contribution to $\rho(T)$ exhibits a maximum value, is compared with theoretical models. It is shown that the experimental results not only depend on a volume effect as given by the compressible Kondo lattice model of Lavagna but in addition confirm the more complex behaviour recently presented by Burdin and Fulde for a Kondo alloy system in which the magnetic (Ce) and non-magnetic (La) atoms are distributed randomly. Non–Fermi–liquid behaviour is predicted by Burdin and Fulde at certain critical concentrations of the alloy system and experimental evidence for this is presented through $\chi(T)$, $\rho(T)$ and $C_P(T)$ measurements.

1. Introduction

The equiatomic ternary compounds CePtIn [1], CePdIn [2] and CeNiIn [3, 4] crystallise in the hexagonal ZrNiAl structure (space group $P\bar{6}2m$). CePtIn and CePdIn are classified as dense–Kondo materials while CeNiIn shows valence fluctuating behaviour [5]. Heat capacity (C_P) measurements on CePtIn yield $C_P/T \approx 1000$ mJ K^{-2} mol^{-1} at 60 mK [5] and indicate no evidence of magnetic order down to this temperature. The absence of ordered magnetism for this compound is also indicated from electrical resistivity studies down to 50 mK [6]. CePdIn with a marginally larger unit–cell volume than CePtIn (0.2066 nm^3 [2] compared to 0.2063 nm^3 [1]) orders antiferromagnetically at 1.7 K [5]. Kondo temperatures were evaluated for all three compounds using $C_P(T)$ data [5] giving 3.3 K for CePdIn, 11 K for CePtIn and 94 K for CeNiIn which has a considerably smaller unit–cell volume (0.1954 nm^3 [4]) than the other two compounds. Thermopower $S(T)$ measurements on the CeTIn compounds yield large positive values and broad peaks in $S(T)$ at 60 K for CePtIn, 85 K for CePdIn and 130 K for CeNiIn [7].

The present paper is concerned with the properties of the ($Ce_{1-x}La_x$)PtIn alloy system as studied through magnetic susceptibility ($\chi(T)$), electrical resistivity ($\rho(T)$), magnetoresistivity (MR) and heat capacity (C_P) measurements. Kondo energy scales as obtained in this study are shown to depend both on volume and dilution effects for these alloys. The volume effect is discussed in

[#] On leave from the Department of Physical Sciences, South Eastern University, Oluvil, Sri Lanka.

terms of the compressible Kondo lattice (CKL) model [8, 9] while dilution with La leads to results that agree with a very recent theoretical description by Burdin and Fulde [10]. Non–Fermi–liquid (nFL) behaviour is indicated by $\chi(T)$, $C_P(T)/T$ and $\rho(T)$ for particular compositions of the alloy system. The results support the suggestion of nFL behaviour in a scenario presented by the authors of ref. [10] in their theoretical study of randomness in a Kondo alloy.

2. Experimental details

Polycrystalline samples of $(Ce_{1-x}La_x)PtIn$ were prepared by arc–melting stoichiometric amounts of the constituent elements on a water-cooled copper hearth in a titanium gettered ultra–pure argon gas atmosphere. The purities in wt% of the materials used were Ce: 99.98, La: 99.99, Pt: 99.97, and In: 99.999. Room–temperature powder x-ray diffraction (XRD) analyses of the specimens were made in order to establish their crystal structure, confirm their single–phase character and determine their lattice parameters.

Measurements of $\rho(T)$ were performed on all alloys using a standard four-probe dc method between 300 and 4 K. For some selected samples $\rho(T)$ and MR measurements were performed to lower temperatures (down to 1.5 K) using a 8 T magnet, variable temperature insert and a temperature controller manufactured by *Oxford Instruments* and in a 9 T magnet of a Physical Properties Measurement System (PPMS) supplied by *Quantum Design*. Samples for $\rho(T)$ studies were bar shaped and of typical dimensions 6 x 1 x 1 mm^3.

Magnetization and susceptibility measurements were obtained using the vibrating sample magnetometer option of the PPMS with sample temperatures varied and controlled in the range 1.9–400 K. Dimensions of typical samples used in these studies were 3 x 1 x 1 mm^3 and the magnetic field $B=\mu_0 H$ was applied along the long axis of the bar. Heat capacity measurements were performed on some selected samples using the PPMS.

3. Results and discussion

3.1 X-ray diffraction results

The room temperature hexagonal unit–cell parameters a and c and the unit–cell volume V of the alloy compositions $0 \le x \le 1$ of the $(Ce_{1-x}La_x)PtIn$ alloys are shown in figure 1. Lattice parameters were calculated using standard regression analyses of well resolved peaks of the XRD powder spectrum of each alloy. The dashed lines represent least–squares (LSQ) fits to the data and illustrate that Vegard's rule is followed over the complete range of x for this system. Our room–temperature lattice parameters are consistent with the values a=0.7653 nm and c=0.4068 nm reported for CePtIn [1] and a=0.7688 nm and c=0.4129 nm reported for LaPtIn [11] in earlier studies.

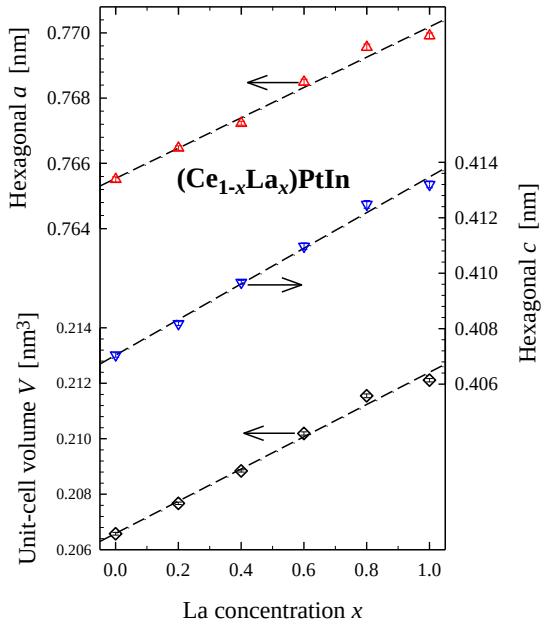

Figure 1. The hexagonal lattice parameters *a* and *c* and unit−cell volume *V* of alloy compositions $0 \le x \le 1$ of the $(Ce_{1-x}La_x)PtIn$ system.

3.2 Electrical Resistivity

Results of $\rho(T)$ for the $(Ce_{1-x}La_x)PtIn$ alloys are depicted in figure 2. Kondo maxima characteristic of dense Kondo behaviour occur at a temperature T_{max}^{ρ} for alloys $0 \le x \le 0.2$. The coherence effects seen for alloys in the dense Kondo region diminish with increasing *x* and for the present system vanish for a critical concentration $x_c \approx 0.2–0.3$, above which single–ion Kondo behaviour is observed. Such a critical concentration is characteristic of Kondo hole systems and is associated with a change in the f–electron density of states $N_f(E_F, x)$ from a two−peak density distribution for the coherent state to a single−peak density distribution for the incoherent state [12–14]. Experimentally x_c is observed to take a wide range of values from e.g. $x_c \approx 0.03$ for $(Ce_{1-x}La_x)Pd_3$ [15] to $x_c \approx 0.7$ for $(Ce_{1-x}Y_x)Pt_2Ge_2$ [16]. The crossover seems to strongly depend on the concentration of f–moments (1–*x*) and the number of delocalised electrons per unit cell, n_c [10, 17].

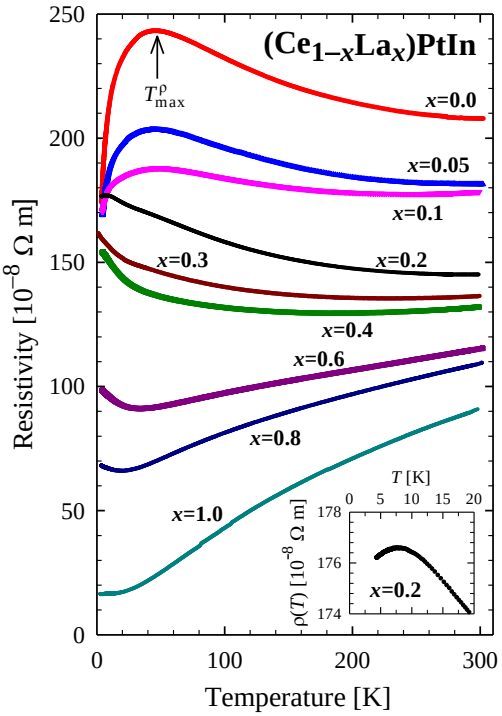

Figure 2. Electrical resistivity $\rho(T)$ for the $(Ce_{1-x}La_x)PtIn$ system ($0 \le x \le 1$).

The magnetic contribution $\rho_{mag}(T)$ to the resistivity is obtained by subtracting the phonon resistivity as given by the experimental resistivity results for the LaPtIn compound: $\rho_{mag}(T)=\rho(T)-(\rho_{LaPtIn}(T)-\rho_{LaPtIn}(0))$. The magnetic resistivities for alloy compositions $0 \le x \le 0.8$ of the $(Ce_{1-x}La_x)PtIn$ system are depicted in figure 3. All alloys exhibit at higher temperatures a logarithmic increase in $\rho_{mag}(T)$ with decrease in temperature as expected for Kondo systems. This is shown by the solid line LSQ fits of the equation

$$\rho_{mag}(T) = A - C_K \ln T \qquad (1)$$

to the experimental data. The coefficient A obtained from the LSQ fits includes in addition to a temperature independent Kondo contribution, also the residual resistivity due to defects and this could be different for each of the alloy samples. Values of A and C_K from the LSQ analyses, as well as the temperatures $T^{\rho(mag)}_{max}$ where $\rho_{mag}(T)$ attains its maximum value (see figure 3) are given in table 1.

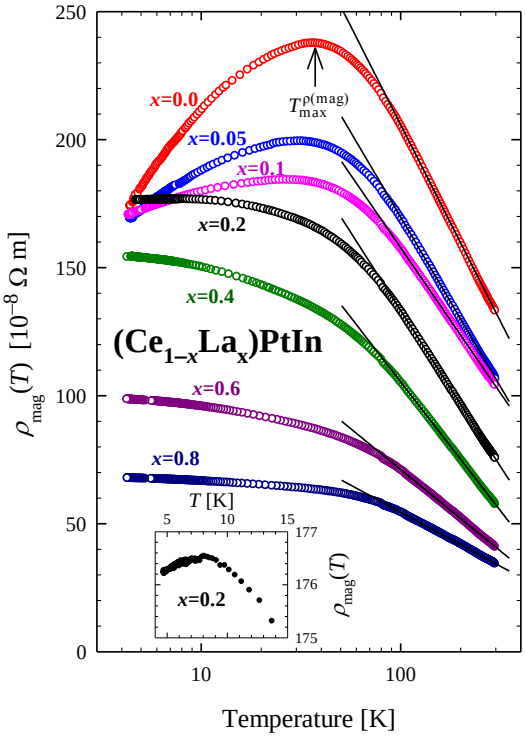

Figure 3. The magnetic contribution to the resistivity $\rho_{mag}(T)=\rho(T)-(\rho_{LaPtIn}(T)-\rho_{LaPtIn}(0))$ for the $(Ce_{1-x}La_x)PtIn$ alloys ($0 \le x \le 0.8$). The solid lines represent the $\rho_{mag}(T) \propto -\ln T$ behaviour observed at high temperature.

Table 1. A and C_K values extracted from LSQ fits of (1) as shown by solid lines in figure 3, as well as $T_{max}^{\rho(mag)}$ values obtained from figure 3.

x	A [10^{-8} Ω m]	C_K [10^{-8} Ω m]	$T_{max}^{\rho(mag)}$ [K]
0.0	513.0(6)	66.7(1)	36.4
0.05	434.6(5)	57.5(1)	31.7
0.1	384.9(3)	49.3(1)	26.9
0.2	376.9(3)	52.9(1)	8.0
0.4	306.8(2)	43.73(4)	–
0.6	198.5(2)	27.64(4)	–
0.8	139.0(2)	18.35(3)	–

3.3 Magnetization and susceptibility

Figure 4 shows the magnetization σ for a selected number of isotherms for the CePtIn parent compound as well as for those alloys for which it is shown in section 3.6 that they exhibit nFL behaviour in their susceptibility, electrical resistivity and heat capacity. No evidence is found for metamagnetic behaviour in the $(Ce_{1-x}La_x)PtIn$ system in contrast with such behaviour observed for CePtGa, $Ce(Pt_{1-x}Ni_x)Ga$ and $CePt(Ga_{1-x}Al_x)$ alloys [18].

Susceptibility data taken in B=0.1 T conform with Curie–Weiss behaviour at higher temperatures. This is indicated in figure 5 by the LSQ fits (solid lines) of the $\chi^{-1}(T) = 3k_B(T-\theta_P)/N_A\mu_{eff}^2$ relation to the experimental data. Resulting values of μ_{eff} and $-\theta_P$ are given in table 2. Values of $-\theta_P$ decrease with increase in x as shown in the inset to figure 5.

The μ_{eff} and $-\theta_{\text{P}}$ values obtained for CePtIn are slightly higher than the values 2.58 μ_{B} and 73 K previously reported in literature [19].

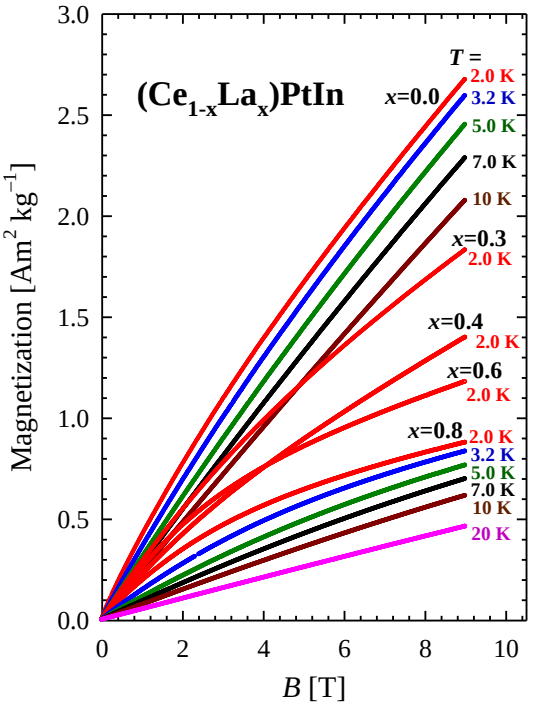

Figure 4. Magnetization σ as a function of applied field $B=\mu_0 H$ for the $(Ce_{1-x}La_x)PtIn$ alloys $(0 \le x \le 0.8)$.

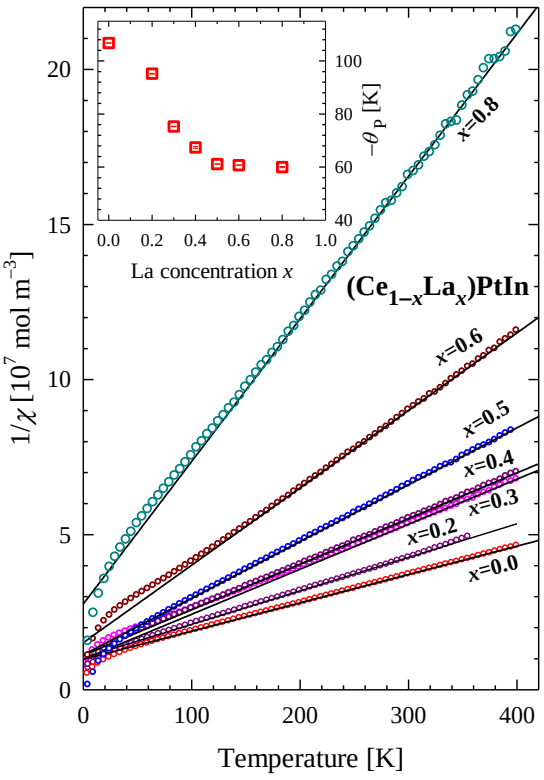

Figure 5. Inverse magnetic susceptibility $\chi^{-1}(T)$ versus temperature for the $(Ce_{1-x}La_x)PtIn$ system illustrating Curie–Weiss behaviour (solid lines). For sake of clarity the data set has been depopulated in the figure by plotting one in every 50 measured points. However, all measured points are used in the LSQ analysis. The insert gives the temperature dependence of $-\theta_P$ where θ_P is the Weiss constant.

Table 2. The Weiss constant θ_P and effective magnetic moment μ_{eff} as obtained by LSQ fits of the Curie–Weiss relation to the $\chi^{-1}(T)$ data in figure 5.

x	$-\theta_P$ [K]	μ_{eff} [μ_B]	Fitted range
0.0	106.75(4)	2.84(2)	400-120 K
0.2	95.2(1)	2.72(4)	350-120K
0.3	75.3(1)	2.52(3)	400-120K
0.4	67.4(3)	2.53(5)	400-120K
0.5	61.1(1)	2.38(2)	400-140 K
0.6	60.7(1)	2.21(3)	400-140 K
0.8	60.0(2)	1.89(3)	400-160 K

3.4 Magnetoresistivity

Magnetoresistance (MR) isotherms were measured in transverse fields up to 8 T for the alloys x=0.4 and x=0.6 and up to 9 T for the alloys x=0.2 and x=0.3. A typical example of the results is shown in figure 6 for the $(Ce_{0.7}La_{0.3})PtIn$ alloy and it is noted that no hysteresis was observed from the results of increasing and decreasing field runs. The experimental results conform with the results of the Bethe ansatz calculations of the Coqblin-Schrieffer model as given by Schlottmann [20]

$$\frac{\rho(B)}{\rho(0)} = \left[\frac{1}{2j+1} \sin^2\left(\frac{\pi n_f}{2j+1} \right) \sum_{\ell=0}^{2j} \sin^{-2}(\pi n_\ell) \right]^{-1} \qquad (2)$$

as shown by the LSQ fit of (2) for the $j = \frac{1}{2}$ case against the experimental isotherms (solid lines in the main figure). Exact solutions for $j = \frac{1}{2}$ in the Schlottmann formalism indicate that the MR is completely determined by a characteristic field B^* [20] which is expected to have the following temperature dependence [21]

$$B^*(T) = B^*(0) + \frac{k_B T}{g\mu_K} = \frac{k_B (T_K + T)}{g\mu_K} . \qquad (3)$$

$B^*(T)$ values obtained from the LSQ fits of (2) to the $\rho(T,B)/\rho(T,0)$ data for the various isotherms, are plotted in the inset in figure 6. A LSQ fit of (3) to the $B^*(T)$ points gives $B^*(0)$ and hence T_K and the magnetic moment μ_K of the Kondo ion. Values of T_K and μ_K obtained for the x=0.2, 0.3, 0.4 and 0.6 alloys are given in table 3. The observed values of μ_K are significantly reduced from the paramagnetic μ_{eff} values given in table 2. The variation of T_K with x is discussed in section 3.5.

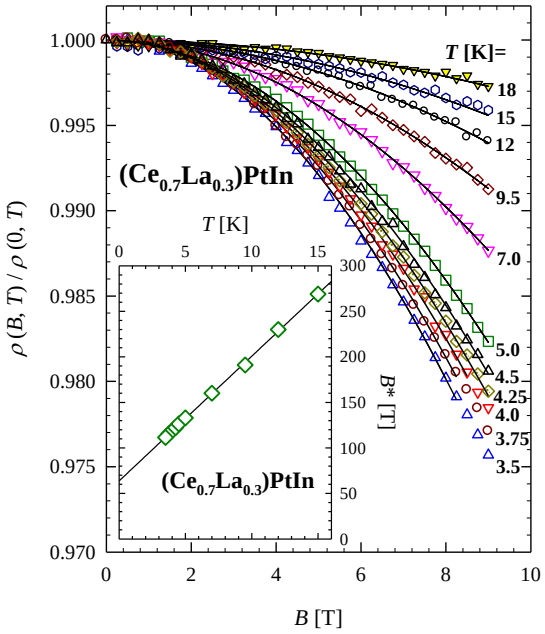

Figure 6. Magnetoresistance isotherms for $(Ce_{0.7}La_{0.3})PtIn$ are given in the main figure and LSQ fits of the Schlottmann equation (2) to the data lead to $B^*(T)$ values as described in the text. The $B^*(T)$ values as depicted in the inset are used to find the Kondo temperature T_K and Kondo moment μ_K by a fit of (3) to the $B^*(T)$ values.

Table 3. Values of the Kondo temperature T_K and the magnetic moment of the Kondo ion μ_K as obtained from fits of equations (2) and (3) to the magnetoresistance data of the $(Ce_{1-x}La_x)PtIn$ alloys.

x	T_K [K]	μ_K [μ_B]
0.2	4.78(8)	0.0291(3)
0.3	4.7(1)	0.0544(7)
0.4	5.6(4)	0.062(2)
0.6	0.6(6)	0.036(3)

3.5 Dilution and volume dependence of T_K

The compressible Kondo lattice (CKL) model for Ce compounds [8, 9] gives the volume dependence of $|J\,N(E_F)|$ as $|J\,N(E_F)| = |J\,N(E_F)|_0 \exp[-q(V-V_0)/V_0]$, where $|J\,N(E_F)|_0$ indicates the value of the quantity at an initial volume V_0. Furthermore, q refers to the Grüneisen parameter of $|J\,N(E_F)|$ (i.e. $q = -\partial \ln |JN(E_F)| / \partial \ln V$) and it is considered to vary between 6 and 8 [9, 22]. Since $T_{max}^{\rho(mag)} \propto T_K \propto \exp\left(-1/|JN(E_F)|\right)$ the volume dependence of T_{max} may be described by

$$\frac{T_{max}^{\rho(mag)}(V)}{T_{max}^{\rho(mag)}(V_0)} = \exp\left[\frac{q\,(V_0 - V)}{|J\,N(E_F)|_0\,V_0}\right] = \exp\left[\frac{\kappa_0 q P}{|J\,N(E_F)|_0}\right] \quad (4)$$

as a function of the concentration dependent volume V or hydrostatic pressure P as done in many such studies in the literature [22–25]. The compressibility is denoted by κ_0. Figure 7 shows a plot

of $T_{max}^{\rho(mag)}(V)/T_{max}^{\rho(mag)}(V_0)$ and $T_K^{MR}(V)/T_{max}^{\rho(mag)}(V_0)$ against $(V-V_0)/V_0$. Furthermore, (4) is fitted to the hydrostatic pressure dependence values of $T_{max}^{\rho(mag)}$ of CePtIn given in ref. [26] as indicated by a solid line in figure 7. Since the compressibility of CePtIn is not known we used a value of κ_0 =6.25 x 10^{-4} $(kbar)^{-1}$ for it as deduced for the related compound CePtGa by scaling the pressure dependence of T_N as obtained from a direct hydrostatic pressure experiment with a chemical pressure experiment on CePtGa [18]. Such a value of κ_0 is comparable to κ_0 values for other heavy–fermion or dense Kondo compounds [27]. The hydrostatic pressure results are extrapolated in figure 7 to negative pressures using (4) as shown by a dashed line. This can be regarded as an approximate reference for the volume contribution to $T_{max}^{\rho(mag)}$ of the $(Ce_{1-x}La_x)PtIn$ system. It is clear that the Kondo energy scale of the $(Ce_{1-x}La_x)PtIn$ system as manifested by $T_{max}^{\rho(mag)}$ and plotted in figure 7 shows a more rapid decrease than expected from the volume (pressure) effect. This additional contribution to the decrease of $T_{max}^{\rho(mag)}$ is ascribed to the dilution effect of La substitution in the Ce sublattice (Kondo hole effect) as has been illustrated in the $(Ce_{1-x}La_x)Pt_2Si_2$ alloy system [28] and also as reported in some theoretical studies [13, 14, 29]. In view of the uncertainty in the value of κ_0 for CePtIn we refrain from using the extrapolated dotted line in figure 7 to obtain through subtraction the dilution dependence of T_K ($\approx T_{max}^{\rho(mag)}$).

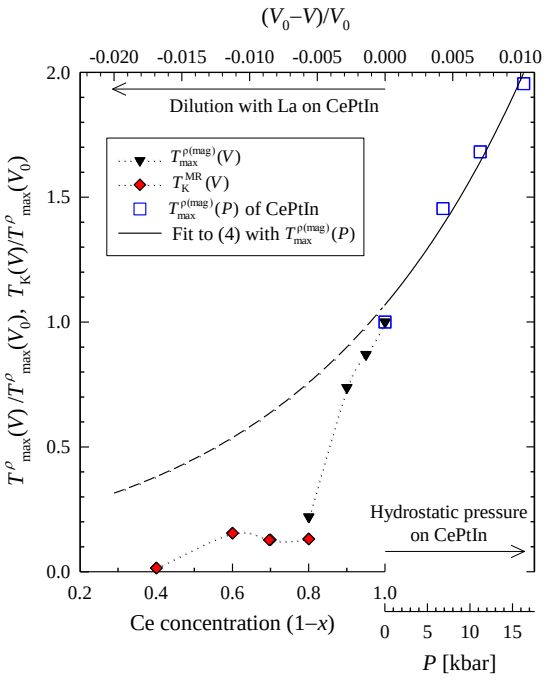

Figure 7. Plot of the change in the Kondo energy scale of the $(Ce_{1-x}La_x)PtIn$ system $0.4 \le 1-x \le 1.0$ upon dilution and of CePtIn upon application of hydrostatic pressure [26] compared with the CKL model equation (4) (solid and dashed lines). The plot is made against Ce concentration $(1-x)$ on the x–axis in order to compare the Kondo energy scale of the $(Ce_{1-x}La_x)PtIn$ system with figure 6 in ref [10]. The solid line gives a LSQ fit of equation (4) to the $T_{max}^{\rho(mag)}(P)$ data of CePtIn from ref. [26] and the dashed line is an extrapolation of this curve to negative pressures.

Theoretical studies by Kaul and Vojta [17] and Burdin and Fulde [10] investigated the effects due to randomly placed Kondo ions in a lattice as a result of dilution by a non–magnetic ion. These studies show that the crossover between the dilute impurity regime and the dense Kondo regime

occurs when the concentration of *f*–moments n_f (i.e. (1–*x*)) is equal to the number of delocalized electrons per unit cell n_c. Kaul and Vojta show that in a region in the vicinity of $n_f \approx n_c$ the system is characterized by inhomogeneities causing nFL behaviour due to a subtle interplay of disorder and strong electronic correlations [17]. Recently Burdin and Fulde [10] described the effect of dilution on the Kondo temperature T_K by considering the effect of randomness in Kondo alloys in which hopping of electrons takes place either between Ce and La sites or between Ce sites themselves or alternatively between La sites (the A and B sites of their paper). A dimensionless quantity α which compares the energies characterizing these two possibilities, as well as the electron filling parameter n_c, enters the theory. When $\alpha > 1$ it is predicted that there are two critical concentrations of Ce–ions, x_{c1} and x_{c2}, in the vicinity of which T_K is considerably reduced (see figures 6(c), 6(d) and 7 in [10]). The variation of the Kondo energy scale with Ce concentration as observed for $(Ce_{1-x}La_x)PtIn$ from magnetoresistance measurements and $T_{max}^{\rho(mag)}$ values in figure 7 shows close similarity to the calculated results obtained by Burdin and Fulde for the $\alpha > 1$ case. In particular the rapid drop in $T_{max}^{\rho(mag)}$ values between (1–*x*)=1.0 and 0.8 observed in the experimental measurements is also seen in the calculated T_K values for the α=3 case [10]. It should also be mentioned that in view of the dramatic drop in $T_{max}^{\rho(mag)}$ between (1–*x*)=1.0 and 0.8, MR studies have also been performed for the (1–*x*)=1.0 and 0.9 alloys which are clearly in the dense Kondo region and for the (1–*x*)=0.8 sample which is in the region where the dense Kondo behaviour changes to dilute Kondo behaviour. All isotherms measured between 2 and 45 K for the (1–*x*)=1.0 and 0.9 alloys showed positive magnetoresistance which is in accordance with the theoretical expectations of Kawakami and Okiji [30] for a Kondo lattice in certain regions of the (B, T_K) parameter space. Therefore the Schlottmann analysis could not be applied to these data in order to obtain T_K values and hence an independent measure of the Kondo energy scales for these concentrations. Isotherms for the (1–*x*)=0.8 alloy gave negative magnetoresistance of similar shape as shown in figure 6 for the (1–*x*)=0.7 alloy. T_K and μ_K values for the (1–*x*)=0.8 alloy are included in table 3 and the observed T_K value is in fair agreement with the corresponding $T_{max}^{\rho(mag)}$ value as is indicated in figure 7. It is observed in figure 7 that the two critical concentrations indicated in ref. [10] appears at $(1-x)=x_{c2} \approx 0.75$ and $(1-x)=x_{c1} \approx 0.4$ for our alloy system (with the Ce concentration indicated by (1–*x*) in our notation, whereas it is indicated by *x* in ref. [10]). Burdin and Fulde suggest the possibility of nFL behaviour in the vicinity of the critical points x_{c1} and x_{c2}. Our measurements of $\chi(T)$, $\rho(T)$ and $C_P(T)$, as discussed in the next section, indicate characteristic nFL behaviour for alloys (1–*x*)=0.7 and 0.6, thus corroborating the theoretical expectations of such effects.

3.6 Non–Fermi–liquid behaviour

Non–Fermi–liquid behaviour has been reported for many f–electron systems and the experiments show a variety of temperature dependences for $C_P(T)/T$, $\chi(T)$ and $\rho(T)$ [31]. Extensive theoretical models exist that attempt to explain the deviations from Landau Fermi–liquid behaviour and these are treated in several reviews: Multichannel Kondo models [32–34], quantum phase transitions [35] and disorder–induced nFL theories [36]. The theoretical work predicts a number of possible temperature behaviours, most notable power–law or logarithmic temperature dependencies of the above mentioned material properties.

Figure 8 illustrates the occurrence of nFL behaviour in $\chi(T) = \sigma(T)/B$ measurements of selected alloys in the $(Ce_{1-x}La_x)PtIn$ system. It is seen that $\chi(T)$ for the *x*=0.3 alloy conforms for measurements taken in B=0.1 T to a power–law for more than a decade in temperature. The *x*=0.4 alloy does not follow a power–law fit for B=0.1 T but follows such behaviour over a smaller temperature range for an applied field of 1 T. The power–law behaviour in figure 8 is expressed in the form $\chi = AT^{-1+\lambda}$ as proposed by Castro Neto *et al* in their Griffiths phase description of

disordered Kondo alloys [37] and which is the form used by Stewart in his review paper to describe nFL alloys that conform to a power–law description. The fits indicated by dashed lines in figure 8 give A=2.137(2) and λ=0.6502(4) for the B=0.1 T data of the x=0.3 alloy, and A=1.555(1) and λ=0.6791(6) for the B=1 T data of the x=0.4 alloy. For λ<1 the heat capacity is expected to be proportional to T^{λ} according to Castro Neto *et al* [37]. Our C_P^{mag}/T data depicted in figure 9 for the x=0.3 and x=0.4 alloys follow a logarithmic rather than a power–law behaviour over more than a decade in temperature. It is seen in figure 9 that some deviation from a logarithmic dependence appears at the lowest investigated temperatures. This could be the start of a flattening of C_P^{mag}/T at lower temperatures as has been observed in the $UCu_{5-x}Pd_x$ system (x=1.0, 0.8) for which an abrupt flattening occurs below some low temperature point after following a logarithmic temperature dependence above this temperature [38]. This levelling off behaviour was associated with either antiferromagnetic order or existence of spin clusters at low temperatures in the $UCu_{5-x}Pd_x$ system. Measurements to lower temperatures are needed to ascertain the behaviour for our system. A fit of $C_P^{\mathrm{mag}}/T = \gamma_0 \ln(T_0/T)$ to the experimental data are indicated by solid lines in figure 9 and yield γ_0=0.109(1) J K^{-2} (mol Ce)$^{-1}$ and T_0= 53(1) K for the x=0.3 alloy and γ_0=0.0878(5) J K^{-2} (mol Ce)$^{-1}$ and T_0= 95(1) K for the x=0.4 alloy. It is noted that the results for the two alloy compositions both scaled per mol Ce does not fall on a universal curve thus indicating that the nFL behaviour is not strictly a single–ion property for this system. The effect of applying a 9 T field is indicated for both alloys in figure 9. One would expect that a sufficiently large applied field should recover Fermi–liquid behaviour resulting in temperature independent values for C_P^{mag}/T at low temperatures (see for instance such behaviour in nFL $CeCu_{5.9}Au_{0.1}$ [39]). Our 9 T results below 3 K give some suggestion that the C_P^{mag}/T curves may tend to temperature independent values at low temperature but measurements down to the mK region are required to establish if such Fermi–liquid behaviour is recovered in a field.

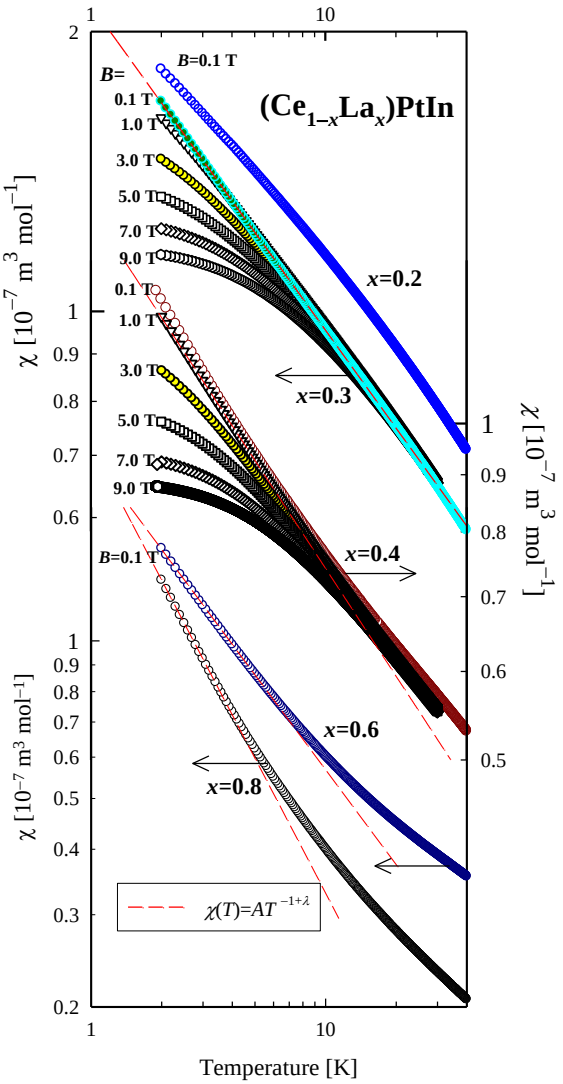

Figure 8. Plot of isofield measurements of $\chi(T)$ of selected alloys of the $(Ce_{1-x}La_x)PtIn$ system ($0 \leq x \leq 0.8$). Non–Fermi–liquid power–law behaviour is observed for the B=0.1 T curve of the x=0.3 alloy over two decades in temperature and to a lesser extend for other alloys. The effect of the magnetic field in recovering Fermi–liquid behaviour is illustrated.

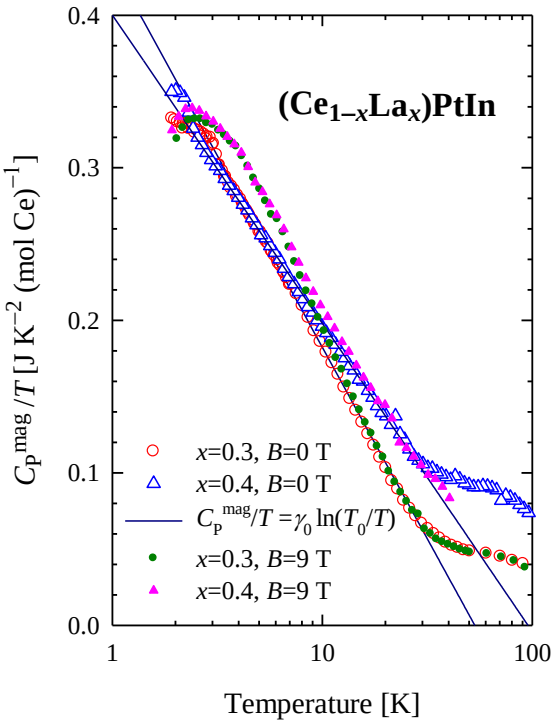

Figure 9. The plot of C_P^{mag}/T at zero and 9 T fields. The magnetic contribution to the specific heat is obtained by subtracting the $C_P(T)$ of LaPtIn.

Figure 10 depicts the temperature dependence of $\rho_{mag}(T)$ at low temperatures in B=0 for several alloy compositions $0.3 \le x \le 0.8$, as well as isofield $\rho_{mag}(T)$ values for the x=0.3 alloy in several fields. Furthermore, for the x=0.4, 0.6 and 0.8 alloys isotherm curves obtained in the MR experiments have been used to calculate $\rho_{mag}(T)$ results for B=4 and 8 T. It is observed that the B=0 curve of the x=0.4 alloy shows a near–linear temperature dependence over almost a decade towards the lowest temperature available for our investigation. LSQ fits of the equation

$$\rho_{mag}(T) = \rho_0\left(1 - bT^n\right) \tag{5}$$

to the low temperature data points for zero–field in the x=0.3, 0.4 and 0.8 alloys and for isofield curves at B=1, 2 and 5 T for the x=0.3 alloy give the fit parameters as tabulated in table 4. These fits show power–law behaviour with n<2, which is characteristic of nFL behaviour. As seen for the x=0.3 alloy, sufficiently large fields tend to destroy the nFL behaviour. As illustrated in the inset to figure 10 for x=0.3, n increases with applied filed and by extrapolation it would reach the single–impurity Fermi–liquid value of n=2 in an applied field of B=6.4 T. Further increase of B takes the alloy to the dense Kondo regime with coherence peaks observed in $\rho_{mag}(T)$ for both the B=7 T and 9 T curves. Larger fields than these as well as lower temperatures are needed to completely recover coherent heavy Fermi–liquid behaviour $\rho_{mag}(T) = \rho_0\left(1 + bT^2\right)$ (with b>0).

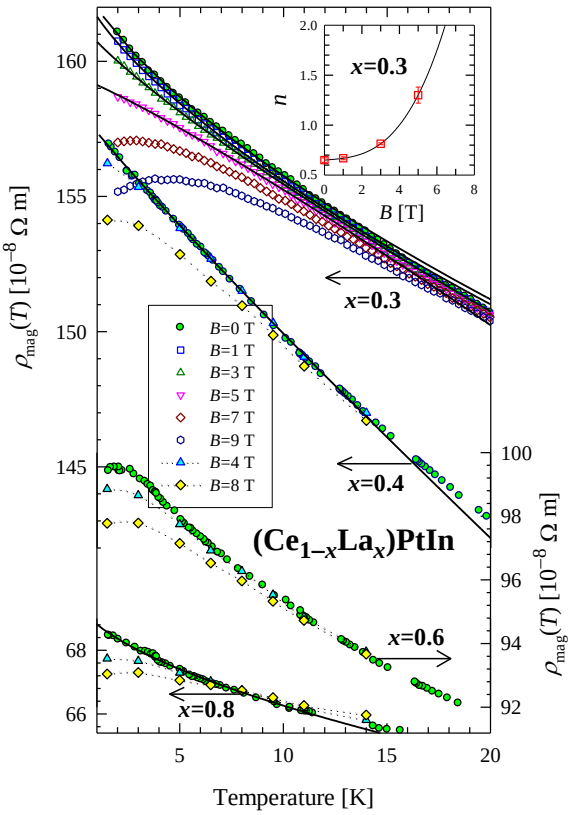

Figure 10. Plot of field–dependent $\rho_{mag}(T)$ measurements for alloy compositions $0.3 \le x \le 0.8$ of **the** $(Ce_{1-x}La_x)PtIn$ system. The solid line fits are to (5).

Table 4. Results of the LSQ fits to (5) for the experimental data of the x=0.3, x=0.4 and x=0.8 alloys.

x	B [T]	ρ(0) [10^{-8} Ω m]	b [K^{-n}]	n
0.3	0	163.8(2)	0.011(4)	0.65(2)
0.3	1	163.3(1)	0.010(2)	0.67(1)
0.3	3	161.68(5)	0.006(1)	0.81(1)
0.3	5	159.21(7)	0.0013(2)	1.30(8)
0.4	0	158.37(6)	0.0065(2)	0.92(1)
0.8	0	69.7(2)	0.013(2)	0.57(5)

Figure 11 illustrates the $\rho_0 - \rho_{mag}(T) \propto T^n$ behaviour over two decades of temperatures for the x=0.3 and x=0.4 alloys. These plots have been affected using the ρ_0 values extracted from the LSQ fits to (5). For all the alloys for which nFL behaviour in $\rho(T)$ have been identified it is seen that (5) is complied with down to the lowest temperatures studied (2 K for x=0.3 alloy and 1.5 K for the other alloys). Further experiments are required to establish the validity of (5) to lower temperatures.

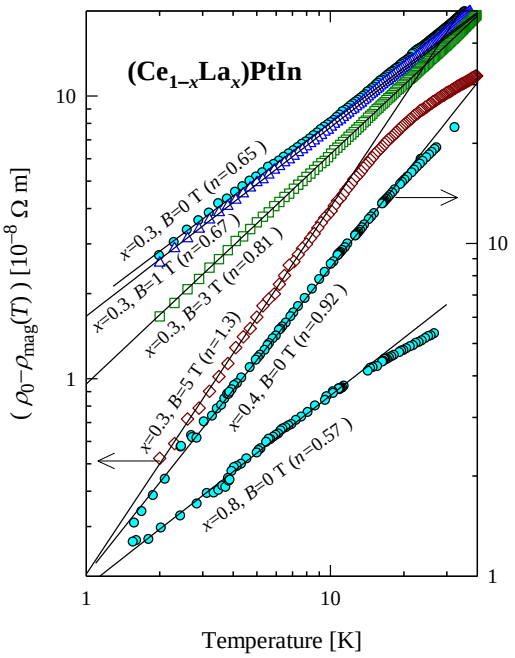

Figure 11. The plot illustrates the linear $\rho_0 - \rho_{\mathrm{mag}}(T) \propto T^n$ behaviour with n<2 at zero–field for the x=0.3, 0.4 and 0.8 alloys and at 1, 3 and 5 T fields for the x=0.3 alloy.

The observation of nFL behaviour in $\chi(T)$, $\rho(T)$ and C_P^{mag}/T for the x=0.3 and 0.4 alloys confirms the anticipated nFL behaviour for alloys near x_{c2} according to the theoretical work in references [17] and [10]. Moreover, nFL behaviour over a more limited temperature region is observed for $\chi(T)$ of the x=0.6 and 0.8 alloys with λ=0.398(2) and λ=0.145(8) respectively, and for $\rho_{\mathrm{mag}}(T)$ of the x=0.8 alloy and these may be associated with the proximity to x_{c1}. It is noted that the predictions of Castro Neto *et al* require robust self–consistency of λ values obtained from susceptibility, heat capacity, frequency dependent susceptibility and the frequency dependent NMR relaxation rate. On the other hand it is known that nFL behaviour is not necessarily observed in each one of the various material properties for a particular system, e.g. for $U(Pt_{0.94}Pd_{0.06})_3$, C_P^{mag}/T exhibits a nFL logarithmic temperature dependence while $\rho(T)$ and $\chi(T)$ show Fermi–liquid behaviour [40]. Our experiments give divergent results for $\chi(T)$ (power–law behaviour) and C_P^{mag}/T (logarithmic behaviour) thus indicating the need for further theoretical analysis to describe such a Kondo–hole system.

4. Conclusion

A study of electrical resistivity and magnetoresistivity on the $(Ce_{1-x}La_x)PtIn$ system indicate that the Kondo energy scale as determined across the alloy series depends on both the volume effect as described by the compressible Kondo lattice model [8, 9] and an effect directly attributed to La dilution [13, 14, 29]. In particular consideration of effects of randomness in the Kondo lattice [10] leads to a theoretical prediction of a significant additional decrease in T_K with La alloying and a more complex behaviour for $T_K(x)$ as given by previous models. Non–Fermi–liquid behaviour is suggested by the theoretical work [10, 17] near certain critical alloy concentrations. Our experimental studies give evidence of a more complex behaviour for $T_K(x)$ and indicate nFL behaviour in resistivity, susceptibility and heat capacity results down to the temperatures used in our studies. Measurements of the investigated properties to lower temperatures than presently

available to us are called for in order to ascertain the nature of the deviation of the logarithmic temperatures dependence of C_P^{mag}/T seen around 2 K and to establish how low in temperature the nFL behaviour in $\rho(T)$ and $\chi(T)$ extends.

Acknowledgements

Support by the South African National Research Foundation (NRF) through grants GUN 2053778 and GUN 2072956 and the Universities of the Witwatersrand and of Johannesburg are acknowledged. We thank Dr. M.B. Tchoula Tchokonté for assisting with the x–ray diffraction measurements and Prof. A.R.E.. Prinsloo for help with some of the PPMS measurements. F.C. Ragel wishes to thank the NRF and Wits University for granting bursaries for the study, and the University of Johannesburg for funding visits to its Physics Department. He also extends his appreciation to the South Eastern University of Sri Lanka for granting leave to pursue his research in South Africa.

References

[1] Hermes W, Rodewald Ute Ch, Chevalier B and Pöttgen R 2007 Solid State Science **9** 874 and references therein
[2] Tursina A I, Nesterenko S N and Seropegin Y D 2004 Acta Crys. **E60** i64
[3] Bulyk I I, Yartys V A, Denys R V, Kalychak Ya M and Haris I R 1999 J. Alloy Compds. **284** 256
[4] Yartys V A, Denys R V, Hauback B C, Fjellvåg H, Bulyk I I, Riabov A B and Kalychak Ya M 2002 *J. Alloy Compds.* **330-332** 132
[5] Satoh K, Fujita T, Maeno Y, Uwatoko Y and Fujii H 1990 *J. Phys. Soc. Jpn*. **59** 692
[6] Maeno Y, Takahashi M, Fujita T, Maeno Y, Uwatoko Y, Fujii H and Okamoto T 1987 *Jpn. J. Appl. Phys.* **26** (suppl. 26-3) 545
[7] Yamaguchi Y, Sakurai J, Teshima F, Kawanaka H, Takabataka T and Fujii H 1990 *J. Phys.: Condens Matter* **2** 5715
[8] Lavagna M, Lacroix C and Cyrot M 1982 *Phys. Lett. A* **90** 210
[9] Lavagna M, Lacroix C and Cyrot M 1983 *J. Phys. F: Met. Phys*. **13** 1007
[10] Burdin S and Fulde P 2007 *Phys. Rev. B* **76** 104425
[11] Kaczorowski D, Andraka B, Pietri R, Cichorek T and Zaremba V I 2000 *Phys. Rev. B* **61** 15255
[12] Zheng-zhong Li and Yang Qiu 1991 *Phys. Rev. B* **43** 12906
[13] Wermbter S, Sabel K and Czycholl G 1996 *Phys. Rev. B* **53** 2528
[14] T. Mutou 2001 *Phys. Rev. B* **64** 245102
[15] Lawrence J M, Graf T, Hundley M F, Mandrus D, Thompson J D, Lacerda A, Torikachvili M S, Sarrao J L and Fisk Z 1996 *Phys. Rev. B* **53** 12559
[16] Sampathkumaran E V, Das I and Vijayaraghavan R 1991 *Z. Phys. B –Condensed Matter* **84** 247
[17] Kaul R K and Vojta M 2007 *Phys. Rev. B* **75** 132407
[18] Ragel F C, Du Plessis P de V and Strydom A M 2007 *J. Phys.: Condens. Matter* **19** 506211
[19] Fujii H, Uwatoko Y, Akayama M, Satoh K, Maeno Y, Fujita T, Sakurai J, Kamimura H and Okamoto T 1987 *Jpn. J. Appl. Phys.* **26** (suppl. 26-3) 549
[20] Schlottmann P 1983 *Z. Phys. B: Condensed Matter* **51** 223
[21] Batlogg B, Bishop D J, Bucher E, Golding B Jr., Ramirez A P, Fisk Z, Smith J L and Ott H R 1987 *J. Magn. Magn. Mater* **63 & 64** 441
[22] Kagayama T, Oomi G, Takahashi H, Mōri N, Ōnuki Y and Komatsubara T 1991 *Phys. Rev. B* **44** 7690
[23] Kagayama T and Oomi G 1993 *Transport and Thermal Properties of f-Electron Systems*, ed G. Oomi *et al* (New York: Plenum Press) p 155
[24] Bauer E, Hauser R, Gratz E, Payer K, Oomi G and Kagayama T 1993 *Phys. Rev. B* **48** 15873
[25] Umeo K, Kadomatsu H and Takabatake T 1996 *Phys. Rev. B* **54** 1194
[26] Kurisu M, Takabatake T and Fujii H 1990 *J. Magn. Magn. Mater.* **90 & 91** 469
[27] Thompson J D and Lawrence J M 1994 *Handbook on the Physics and Chemistry of Rare Earths* vol 19 ed K A Gschneidner Jr, Eyring LeRoy, G H Lander and G R Choppin (Amsterdam:Elsevier) p 383
[28] Ragel F C, du Plessis P de V and Strydom A M 2008 *J. Phys.: Condens. Matter* **20** 055218
[29] Grenzebach C, Anders F B, Czycholl G and Pruschke T 2006 *Phys. Rev. B* **74** 195119
Grenzebach C, Anders F B, Czycholl G and Pruschke T 2008 *Phys. Rev. B* **77** 115125

[30] Kawakami N and Okiji A 1986 *J. Phys. Soc. Japan* **55** 2114
[31] Stewart G R 2001 *Rev. Mod. Phys.* **73** 797
[32] Schlottmann P and Sacramento P D 1993 *Adv. Phys.* **42** 641
[33] Cox D L and Jarrell M 1996 *J. Phys.: Condens. Matter* **8** 9825
[34] Cox D L and Zawadowski A 1998 *Adv. Phys.* **47** 599
[35] Sachdev S 1999 Quantum Phase Transitions (Cambridge: Cambridge University Press)
[36] Miranda E and Dobrosavljević V 2005 *Rep. Prog. Phys.* **68** 2337
[37] Castro Neto A H, Castilla G and Jones B A 1998 *Phys. Rev. Lett*. **81** 3531
Castro Neto A H and Jones B A 2000 *Phys. Rev. B* **62** 14975
[38] Sheidt E-W, Schreiner T, Heuser K, Koerner S and Stewart G R 1998 *Phys. Rev. B* **58** R10104
[39] Von Löhneysen H 1996 *J. Phys.: Condens. Matter* **8** 9689
[40] Kim J S, Stewart G R, Butch N P and Maple M B 2008 *Phys. Rev. B* **78** 035130